

Available online at www.sciencedirect.com

SCIENCE @ DIRECT®

Surface & Coatings Technology xx (2005) xxx–xxx

**SURFACE
& COATINGS
TECHNOLOGY**
www.elsevier.com/locate/surfcoat

Near-surface mechanical properties and surface morphology of hydrogenated amorphous carbon thin films

S.N. Kassavetis, S. Logothetidis *, G.M. Matenoglou

Aristotle University of Thessaloniki, Department of Physics, Laboratory for Thin Films - Nanosystems and Nanometrology, GR-54124, Thessaloniki, Greece

Abstract

The study of the near-surface nanomechanical properties of thin films is a very ambitious task and can be accomplished by advanced surface sensitive techniques. Depth-sensing nanoindentation (NI) is a widely used technique for the nanomechanical characterization of thin films, but it has the inherent limitation of the substrate influence to the measured hardness (H) and elastic modulus (E). Thus, sophisticated modeling is required to determine H and E at the surface. On the other hand, surface acoustic methods seem more promising for such a study. Among them, atomic force acoustic microscopy (AFAM) is a scanning probe microscopy technique based on the resonant vibration of the AFM cantilever. In this work, we study the near-surface nanomechanical properties and the surface morphology of soft hydrogenated amorphous carbon (a-C:H) thin films. We use NI, employing the continuous stiffness measurements technique, and AFAM for the imaging of the variations of the surface mechanical properties and the accurate determination of the elastic modulus. We analyze NI data using empirical models in order to estimate near-surface E and H and the results are compared to those obtained by AFAM. From depth-sensing NI, it was found that the a-C:H thin films present “pop-in” events, which are eliminated by changing the deposition conditions e.g. increasing the negative bias voltage to the substrate (V_b). Near-surface H and E of the a-C:H thin films measured with nanoindentation were found to initially increase with increasing $|V_b|$. Further increase of $|V_b|$ has no effect on the E and H values. Finally, by comparing the results from AFAM and NI, we conclude that the obtained values for E by NI are lower for all the a-C:H thin films.

© 2005 Elsevier B.V. All rights reserved.

Keywords: Hydrogenated amorphous carbon; Surface morphology; Nanoindentation; Atomic force acoustic microscopy

1. Introduction

In recent years, several techniques have been developed to study the nanomechanical properties of thin films. Among them, nanoindentation (NI) is a widely used technique for the measurement of the elastic modulus (E) and the hardness (H), either on a single loading–unloading cycle (CI) [1] or during dynamic loading (continuous stiffness measurements, CSM) [2]. In the case of thin and ultra thin films, a limitation to the measurement of the nanomechanical properties with this technique arises from the small thickness of the films and as a consequence the measured values of H and E are affected by the mechanical response of the substrate. The main advantage of CSM technique, compared to CI, is that it provides the H and E values continuously versus the penetration (contact) depth of the indenter. Thus, the appropriate models, which take into account the substrate effect, can be

applied, in order to estimate the real hardness (H_f) and elastic modulus (E_f) values of the surface of the thin films.

In addition, surface acoustic methods seem more promising for the measurement of the nanomechanical properties of the surface. Several scanning techniques were used for the detection of the surface mechanical response to the acoustic waves. Among them near-field techniques, like atomic force microscopy (AFM), provide better lateral resolution compared to optical scanning techniques, which are restricted by Abbe’s principle. In this study we employ atomic force acoustic microscopy (AFAM) [3], a non-destructive technique for the imaging of the variations of the nanomechanical properties of the surface and the quantitative determination of the near-surface elastic modulus. AFAM is based on the vibration at the resonant frequency of an AFM cantilever, which is in continuous contact with the surface of the film, when an external ultrasonic signal is applied to the sample.

Hydrogenated amorphous carbon (a-C:H) thin films are candidate materials for many cutting edge technological applications, such as protective coatings for optical systems, barrier

* Corresponding author. Tel.: +30 2310 998174; fax: +30 2310 998390.
E-mail address: logot@auth.gr (S. Logothetidis).

coatings on flexible polymeric substrates for packaging and heamocompatible thin films for biomedical applications [4–7]. Thus the surface properties, like the morphology and the mechanical properties, are very important for the performance of the final system. In this work, we study the surface morphology and the near-surface nanomechanical properties of a-C:H thin films. The near-surface E_f and H_f values of the samples were estimated, after extracting the substrate effect, from nanoindentation CSM measurements. The surface topography as well as the imaging of the variation of the surface nanomechanical properties was studied using atomic force microscopy and AFAM, respectively. Finally, the E_f values from nanoindentation were compared to those obtained from AFAM measurements.

2. Experimental

Hydrogenated amorphous carbon thin films were deposited on Si (001) substrates, by rf reactive magnetron sputtering of a 99.999% pure graphite target at high vacuum ($P < 10^{-5}$ Pa) conditions. First, the substrates were chemically cleaned and then dry-etched with very low energy Ar^+ ion bombardment before the deposition process. Argon, at 2 Pa partial pressure, and hydrogen, 10% of the total pressure, were used as the carrier and the reactive gas, respectively. The deposition of the a-C:H thin films was realized either without (floating) or with negative bias (V_b) voltage, ranging from -20 V to -100 V, applied to the substrate.

The nanomechanical properties of the thin films were measured using nanoindentation and AFAM. A Nano Indenter XP commercial apparatus was used for nanoindentation experiments. The nanoindenter is placed in an acoustically isolated enclosure, over an antivibration table and is equipped with the appropriate electronics for the CSM measurements [2]. Several indents (8–10), with $30\text{ }\mu\text{m}$ spacing and loading rate 0.05 mN/s , were made at every sample for statistical purposes. Thus, the presented H and E are the mean values. A Berkovich type diamond tip, with 50-nm nominal radius, was used as the indenter.

The near-surface elastic modulus of the a-C:H thin films was also investigated by AFAM, which is a technique based on the scanning probe microscopy (SPM) principles. The main difference with the classical SPM is that the AFAM configuration includes a piezoelectric transducer, with 2.5 MHz central frequency, which is placed below and in contact with the sample. The transducer emits longitudinal acoustic waves which cause out-of-plane vibrations of the sample surface. By setting the SPM probe (cantilever) in contact with the sample surface, we can acquire the so-called acoustic images, which represent the vibration amplitude of the cantilever. The latter vibrates in contact with the sample surface at a fixed frequency, close to the resonance one. The acoustic images of every sample were acquired simultaneously with the topographic ones, in order to study in terms of surface morphology and nanomechanical properties of the exact same surface areas of the samples. We also acquire the cantilever vibration spectra to estimate E_f [8]. Measurements were performed with a SOLVER P47H Scanning Probe Microscope (NT-MDT, NTI Instruments) in ambient en-

vironment, at room temperature. Standard silicon cantilevers with nominal spring constant $k_c = 1\text{ N/m}$, 10 nm nominal radius and typical resonance frequency 20 kHz was used for AFM and AFAM measurements.

3. Results and discussion

The thickness of the studied a-C:H thin films was measured using spectroscopic ellipsometry (SE) in the $1.5\text{--}6.5\text{ eV}$ energy region [9]. The thickness of all the biased a-C:H thin films is $\sim 150\text{ nm}$ and the unbiased one is $\sim 200\text{ nm}$. The surface morphology of the a-C:H thin films was studied by AFM in contact mode. In Fig. 1, the RMS roughness of the surface is shown. The presented results were originated from a $5 \times 5\text{ }\mu\text{m}^2$ scanning area. The RMS roughness (R_a) of the samples was found to decrease with increasing $|V_b|$ from 2.7 to less than 0.3 nm . The high R_a values of the unbiased a-C:H thin films are attributed to the island growth mode. Similar results have been reported for the unbiased non-hydrogenated a-C thin film [10]. The observed reduction with increasing $|V_b|$ is attributed to the re-sputtering process of the species at the surface occurred during the growth of the thin film [10].

Concerning the microstructural characteristics of a-C:H thin films, spectroscopic ellipsometry analysis revealed that the volume fraction of sp^3 -hybridized carbon bonds increased from 40% to 45% with increasing $|V_b|$ [11]. In addition, X-ray Reflectivity (XRR) measurements revealed that the density of the samples increases from 1.1 g/cm^3 ($V_b > 0$) to 1.5 g/cm^3 ($V_b = -100$) [12]. Thus, the a-C:H thin films were expected to be soft ($H < 8\text{ GPa}$) [4]. The presented nanoindentation results below agree with the above assumption.

In Fig. 2(a,b), typical loading–unloading curves from CSM nanoindentation experiments are shown. In the case of the thin films grown without and with $V_b = -20\text{ V}$ applied to the substrate, a pop-in behavior was observed [13]. The pop-in is comprised by a step, which appears in the loading curve as the displacement of the indenter increases, while the load remains constant. The pop-in event indicates that fracture was induced to these samples by the diamond nanoindenter and it is

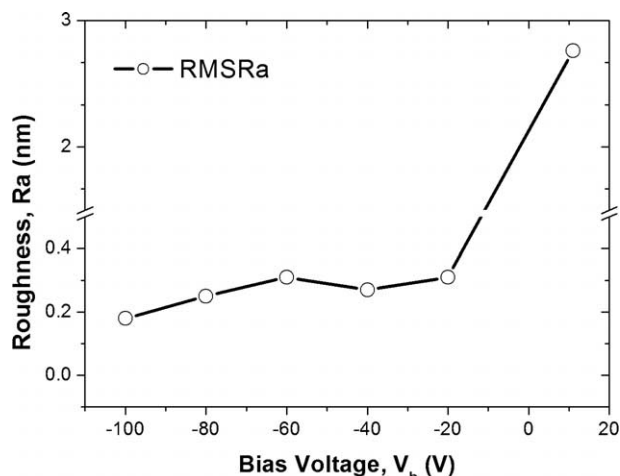


Fig. 1. Evolution of RMS roughness, measured using AFM, vs. bias voltage V_b .

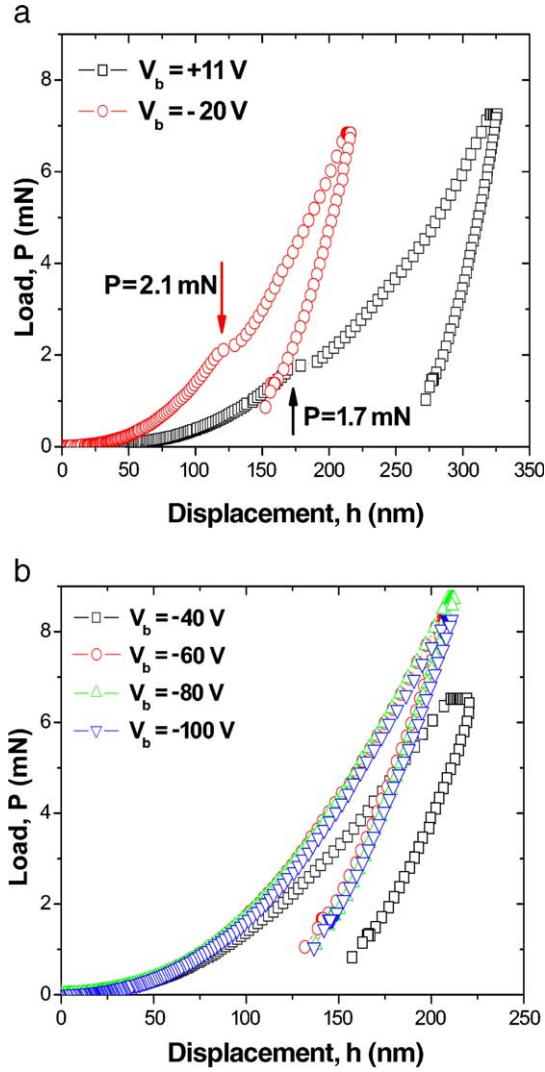


Fig. 2. (a, b) Nanoindentation load–unload curves vs. displacement. Presence (a) and absence (b) of pop-in event in the a-C:H thin films.

detected for 1.7 mN and 2.1 mN applied load P for the floating and the biased ($V_b = -20$ V) a-C:H thin film, respectively. For further increase of $|V_b|$ the pop-in events, which are undesirable for the mechanical performance of the thin film, were eliminated, as evidenced by the absence of any step in the loading curve of these samples (Fig. 2b).

In order to determine the near-surface E_f and H_f values of the a-C:H thin films and to separate the mechanical properties of the films from the substrate influence, the experimental values of E were fitted using Eq. (1), proposed by Doerner and Nix [14], and those of H were fitted using Eq. (2), proposed by Bhattacharya and Nix [15] for the case of soft thin films on harder substrates:

$$\left(\frac{1-\nu^2}{E}\right)_{\text{eff}} = \frac{1-\nu_f^2}{E_f} \left(1 - e^{-\frac{2d}{\sqrt{\pi}h_c}}\right) + \frac{1-\nu_s^2}{E_s} e^{-\frac{2d}{\sqrt{\pi}h_c}}, \quad (1)$$

$$H_{\text{eff}} = H_s + (H_f - H_s) \exp \left[-b \left(\frac{h_c}{d} \right)^2 \right], \quad (2)$$

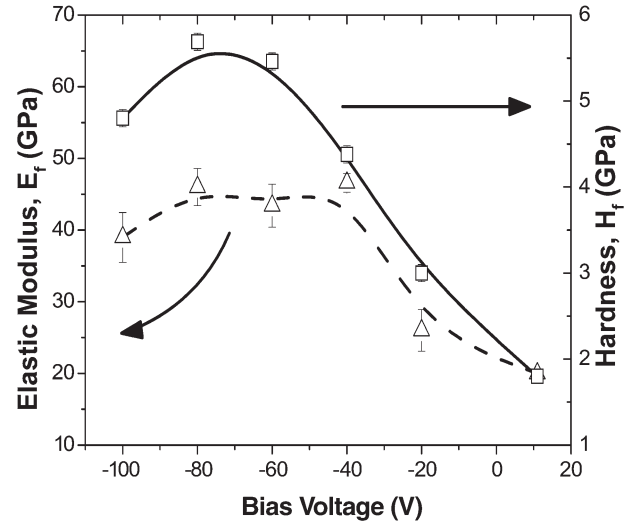


Fig. 3. Effect of substrate bias voltage V_b to the elastic modulus E_f and the hardness H_f .

where ν is the Poisson ratio, h_c the contact depth and α , b were set as free parameters for the fitting procedure [14–16]. E_s and H_s values of the Si(001) substrate were 173 GPa and 12 GPa, respectively, as measured by the CSM nanoindentation. The subscripts s and f denote the substrate and the film, respectively, and eff the measured quantity.

In Fig. 3, the calculated values of E_f and H_f versus the V_b are shown. E_f was found to increase from 20 GPa (floating) to 46 GPa, when $V_b = -40$ V was applied to the substrate. Further increasing of $|V_b|$ do not affect the E_f and a plateau appears in Fig. 3. A similar behavior is also observed for H_f , which is found to increase from 1.8 to 5.6 GPa, when $|V_b| \geq -40$ V. Again a value plateau appears for further increase of $|V_b|$. As it was mentioned above, the values of E_f and H_f are characteristic of the soft a-C:H thin films [4]. In addition, a similar dependence on V_b was also reported for several carbon based (non-hydrogenated, hydrogenated, nitrogenated) thin films [4,17].

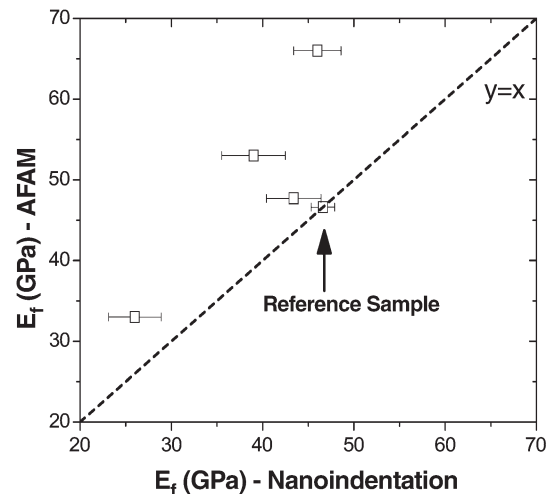


Fig. 4. Elastic modulus E_f of a-C:H measured via nanoindentation and AFAM.

The elastic modulus of the a-C:H thin films was also measured using AFAM technique. A rectangular cantilever, with nominal spring constant $k_c = 1$ N/m, was selected as the scanning probe, in order to apply sufficient low contact force F_c to the soft a-C:H thin films. Cantilevers of the same type were used for all the AFAM scans at every a-C:H thin film. F_c , which is equal to $F_c = k_c \Delta z$, where Δz is the static deflection of the cantilever, was set 140 nN for every scan. In order to estimate the elastic modulus of the samples, the resonant contact frequency f_c of the cantilever and the vibrated surface were measured. The contact stiffness k^* is estimated via f_c [8,18] but for the calculation of the reduced modulus E^* a reference with known elastic modulus is needed. E_f is given by Eqs. (3) and (4) [8,19]:

$$E^* = E_{\text{ref}}^* \frac{k^*}{k_{\text{ref}}^*}, \quad (3)$$

$$\frac{1}{E^*} = \frac{1-\nu_f}{E_f} + \frac{1-\nu_t}{E_t}, \quad (4)$$

where the subscripts t and ref denotes the tip and the reference sample, respectively. In Fig. 4, the E_f estimated by AFAM and nanoindentation is presented. As a reference for the calculation of E_f via AFAM technique, the a-C:H thin film grown with $V_b = -40$ V was used.

Firstly, we observe that the same trend, an increase of E_f with increasing $|V_b|$, appears in AFAM measured E_f . In addition, the values of E_f , for all the a-C:H thin films measured by the AFAM technique, appear to be higher, compared to those obtained by nanoindentation. The discrepancy probably is due to the significant difference between the forces that the probe of every technique applies to the sample, micronewton (μN) in the case of nanoindentation and nanonewton (nN) in the case of AFAM. A similar behavior has been also reported for a-C single layer and multilayer thin films [20], in which the nanoindentation values of the E_f was found to be significantly decreased with respect to the theoretically predicted ones.

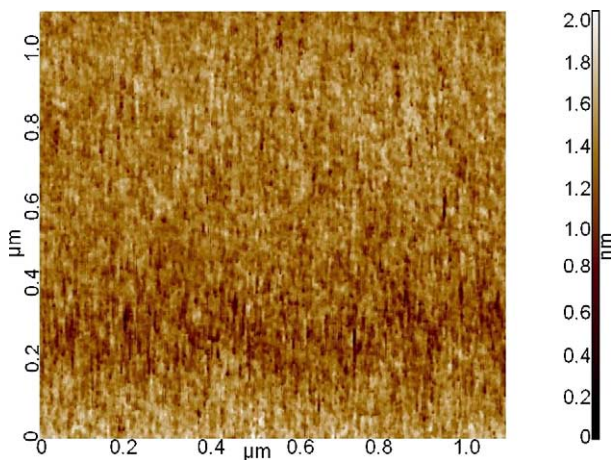


Fig. 5. Topographic image of a-C:H ($V_b = -40$ V) acquired during an AFAM scan.

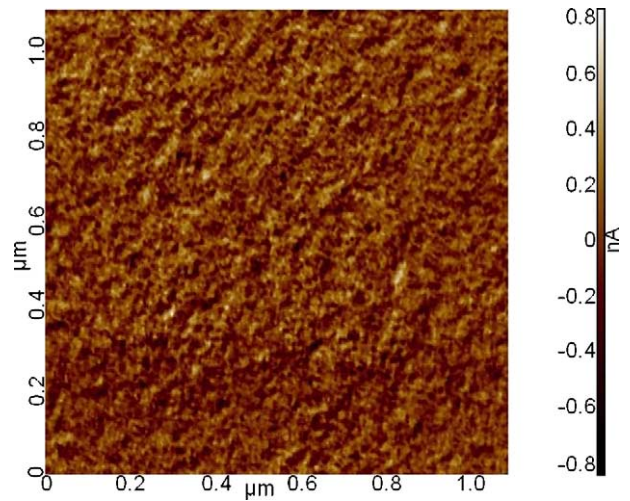


Fig. 6. Acoustic image of a-C:H ($V_b = -40$ V) acquired during an AFAM scan.

A pair of images (acoustic and topographic) of the same area of a representative a-C:H thin film (grown with $V_b = -40$ V) is shown in Figs. 5 and 6. The acoustic image, which is acquired simultaneously with the topographic one during AFAM scan, can provide information about the variations of the nanomechanical properties of the surface. In the acoustic image, the elastic properties of the surface are represented through the amplitude variation. The darker regions in the image correspond to lower contact stiffness and as a consequence to lower E_f values [21]. In the case of this a-C:H thin film, the variations in the acoustic image are different compared to those given by the topographic image. Thus, we assume that the surface morphology did not affect the near-surface elastic properties, which mainly depend on the local network of sp^3 - and sp^2 -hybridized carbon bonds.

4. Conclusions

In this work, we studied the surface morphology and the near-surface mechanical properties of a-C:H thin films. The surface morphology was studied using atomic force microscopy and a decrease of the RMS R_a was found, when we apply a bias voltage to the substrate. “Pop-in” events were detected in the loading NI curve and were eliminated when $V_b \leq -20$ V. The near-surface nanomechanical properties were investigated in the light of nanoindentation and AFAM. The measured H_f and E_f were found to be affected by V_b . E_f increased from 20 to 46 GPa when negative bias voltage is applied to the substrate. H_f was found to increase from 1.8 to 5.6 GPa with increasing $|V_b|$. In addition, the E_f of the samples was measured using AFAM and the E_f values were found higher than those obtained by NI. Finally, imaging of the surface nanomechanical properties was obtained using AFAM.

Acknowledgements

This work has been partially supported by the Greek General Secretariat of Research and Technology under PENED-2001 ED 256 project.

References

- [1] W.C. Oliver, G.M. Pharr, *J. Mater. Res.* 7 (1992) 1564.
- [2] X. Li, B. Bhushan, 48 (2002) 11.
- [3] U. Rabe, K. Janser, W. Arnold, *Rev. Sci. Instrum.* 67 (1996) 3281.
- [4] J. Robertson, *Mater. Sci. Eng., R Rep.* 37 (2002) 129.
- [5] S. Logothetidis, *Thin Solid Films* 482 (2005) 9.
- [6] S. Logothetidis, M. Gioti, S. Lousinian, S. Fotiadou, *Thin Solid Films* 482 (2005) 126.
- [7] M. Yoshida, T. Tanaka, S. Watanabe, M. Shinohara, J.-W. Lee, T. Takagi, *Surf. Coat. Technol.* 174–175 (2003) 1033.
- [8] U. Rabe, S. Amelio, E. Kester, V. Scherer, S. Hirsekorn, W. Arnold, *Ultrasonics* 38 (2000) 430.
- [9] S. Logothetidis, in: H.S. Nalwa (Ed.), *Handbook of Thin Film Technology*, vol. 2, Academic Press, 2002, p. 277.
- [10] S. Logothetidis, M. Gioti, P. Patsalas, *Diam. Relat. Mat.* 10 (2001) 117.
- [11] E. Pavlopoulou, MSc Thesis, Aristotle University of Thessaloniki, 2004.
- [12] P. Patsalas, S. Logothetidis, P.C. Kelires, *Diam. Relat. Mat.* 14 (2005) 1241.
- [13] J. Qi, K.H. Lai, C.S. Lee, I. Bello, S.T. Lee, J.B. Luo, S.Z. Wen, *Diam. Relat. Mat.* 10 (2001) 1833.
- [14] M.F. Doerner, W.D. Nix, *J. Mater. Res.* 1 (1986) 601.
- [15] A.K. Bhattacharya, W.D. Nix, *Int. J. Solids Struct.* 24 (1998) 1287.
- [16] S. Logothetidis, S. Kassavetis, C. Charitidis, Y. Panayiotatos, A. Laskarakis, *Carbon* 42 (2004) 1133.
- [17] A. Laskarakis, S. Logothetidis, C. Charitidis, M. Gioti, Y. Panayiotatos, M. Handrea, W. Kautek, *Diam. Relat. Mat.* 10 (2001) 1179.
- [18] NT-MDT, *Atomic Force Acoustic Microscopy – Instruction Manual*.
- [20] U. Rabe, M. Kopycinska, S. Hiserkorn, J. Munoz Saldana, G.A. Schneider, W. Arnold, *J. Phys., D.* 35 (2002) 2621.
- [21] C. Mathioudakis, P.C. Kelires, Y. Panayiotatos, P. Patsalas, C. Charitidis, S. Logothetidis, *Phys. Rev., B* 65 (2002) 205203.